Title

Germ cells do not progress through spermatogenesis in the infertile zebrafish testis

Authors

Andrea L. Sposato[1], Darren R. Llewellyn[1], Jenna M. Weber[1], Hailey L. Hollins[1], Madison N. Schrock[1], Jeffrey A. Farrell[2], James A. Gagnon[1,3,*]

Affiliations

1. School of Biological Sciences, University of Utah, Salt Lake City, UT 84112
2. Division of Developmental Biology, Eunice Kennedy Shriver National Institute of Child Health and Human Development, NIH, Bethesda, MD 20814
3. Henry Eyring Center for Cell and Genome Science, University of Utah, Salt Lake City, UT 84112

*. Author for correspondence: james.gagnon@utah.edu

Abstract

Vertebrate spermatogonial stem cells maintain sperm production over the lifetime of an animal but fertility declines with age. While morphological studies have greatly informed our understanding of typical spermatogenesis, the molecular and cellular mechanisms underlying spermatogenesis are not yet understood, particularly with respect to the onset of fertility. We used single-cell RNA sequencing to generate a developmental atlas of the zebrafish testis. Using 5 timepoints across the adult life of a zebrafish, we described cellular profiles in the testis during and after fertility. While all germ cell stages of spermatogenesis are detected in testes from fertile adult zebrafish, testes from older infertile males only contained spermatogonia and a reduced population of spermatocytes. These remaining germ cells are transcriptionally distinct from fertile spermatogonia. Immune cells including macrophages and lymphocytes drastically increase in abundance in infertile testes. Our developmental atlas reveals the cellular changes as the testis ages and defines a molecular roadmap for the regulation of male fertility.

Key Words

testis; fertility; spermatogenesis; immune cells; aging; single-cell RNA sequencing

Introduction

The vertebrate testis produces sperm throughout the fertile lifetime of the animal from a population of spermatogonial stem cells. During spermatogenesis, differentiating germ cells undergo transcriptional reprogramming as they mature through a diversity of cell types (Soumillon et al. 2013, Melé et al. 2015). Somatic cells of the testis support spermatogenesis by providing a conducive environment for a balance of germ cell proliferation and differentiation. Several imaging-based strategies have captured the morphology of developing germ and somatic cells, providing insight into the differences in testis composition and organization across species (Maack and Segner 2003, Schulz et al. 2005, Wang et al. 2007, Leal et al. 2009, Uribe et al. 2014, Lee et al. 2017, de Siqueira-Silva et al. 2019).

Mammals and zebrafish share an overall testis architecture composed of several tightly coiled seminiferous tubules (Schulz et al. 2010). As in most animals, spermatogenesis is maintained throughout most of zebrafish adulthood. Unlike mammals, germ cells in zebrafish are not in direct contact with the basement membrane surrounding tubules. Instead, spermatogenesis is a cystic process whereby Sertoli cells surround individual undifferentiated spermatogonia and support their differentiation throughout spermatogenesis (Schulz et al. 2005). Within a Sertoli cyst, germ cells first develop in a clonal syncytium of type A spermatogonia before undergoing 9 mitotic divisions as type B spermatogonia then entering meiosis (Leal et al. 2009). After meiosis, germ cells enter the spermiogenic phase, where spermatids develop into spermatozoa following nuclear condensation, organelle elimination, and formation of the flagellum. The cyst then opens to release mature spermatozoa in the lumen of seminiferous tubules (Schulz et al. 2010). In addition to Sertoli cells, other somatic cell types also serve important roles during spermatogenesis. Leydig cells produce testosterone and insulin-like 3 which promote spermatogenesis via Sertoli cells (Walker 2010, Crespo et al. 2021). A host of immune cells are also present in the testis, including macrophages and various lymphocytes. Regulatory T cells play an important role in immune homeostasis during zebrafish testis development (Li et al. 2020). In mammalian testes, macrophage and lymphocyte populations have also been characterized (Guo et al. 2020, Bhushan et al. 2020) and inflammation has been described as a signature of testicular aging (Matzkin et al. 2016, Nie et al. 2022). To date, the full scope of cell type diversity and plasticity during zebrafish spermatogenesis and aging is not well understood.

Zebrafish become fertile at 3 months old and maintain gametogenesis until about 2 years of age when they are unable to breed or make sperm. We do not know how the cell type composition and transcriptional profiles of the testis may change throughout fertility and the transition to infertility. Single-cell RNA sequencing (scRNAseq) has been used to describe the molecular and cellular composition of testes from several vertebrate and invertebrate organisms. A recent scRNAseq survey profiled the cell types present in 5 month old zebrafish (Qian et al. 2022). As expected, these testes exhibited a continuum of cell types from spermatogonia to elongated spermatids. However, this stage of life marks just the sunrise of a dynamic and continually maintained process throughout the adult life of a zebrafish. Another study compared 18-month testes from control zebrafish and infertile fish that were exposed to an endocrine-disruptive chemical early in life (Haimbaugh et al. 2022). Notably, endocrine disruption caused arrest or apoptosis of post-meiotic germ cells after typical development through spermatogonial and meiotic phases. These results suggest that meiosis acts as a key checkpoint for sperm development. However, profiles of somatic cells are missing from this atlas, and it remains unknown whether this drug-induced post-meiotic apoptosis/arrest is also present in natural cases of infertility. While single timepoint atlases of the zebrafish testis provide snapshots of testicular cell type composition, to probe the mechanisms that control infertility we need to capture the dynamic changes in the testis as fertility declines.

In this study, we describe a developmental atlas of the whole zebrafish testis which characterizes cell types present throughout the fertility window and beyond. We used scRNAseq to profile cell types, enabling us to identify all stages of germ cell differentiation and somatic cells of the testis including Sertoli, Leydig, vascular smooth muscle cells, and immune cells such as macrophages, T cells, and natural killer cells. In naturally infertile testes, we identify a larger and more diverse population of immune cells and an absence of post-meiotic germ cells. While infertile testes are not depleted of germ cells, these germ cells adopt a distinct transcriptional state and do not develop beyond meiotic stages. Our developmental atlas provides insights regarding the maintenance and breakdown of fertility with cellular and molecular resolution.

Results

Timecourse scRNAseq identifies cell types present in the zebrafish testis throughout fertility

To define the cellular composition of zebrafish testes during fertility, we dissected whole testes from fertile adult zebrafish at four ages (5, 12, 20, and 22 months old), dissociated whole tissue, and profiled each sample by scRNAseq (Fig. 1A, S1A). Representative histological images of fertile zebrafish testes show densely packed seminiferous tubules with germ cells proceeding through spermatogenesis and somatic support cells in the interstitial spaces (Fig. 1B, S2). Rates of transcription are highest in the testis compared to every other organ (Xia et al. 2020), so we filtered for high quality transcriptomes based on the percentage of mitochondrial reads (<5%) and the number of genes detected per cell using a threshold established for each data set based on the interquartile range (Fig. S1C). Next, we integrated the six biological samples from all four timepoints to establish a composite atlas of the fertile zebrafish testes that contains 32,659 cells (Fig. 1C, S1B).

We identified all cell types within this fertile atlas using marker genes (Table 1, Fig S1D). We identified germ cells as they progressed through all stages of differentiation from early spermatogonia to spermatozoa (Fig. 1D). We also discovered small populations of somatic cells such as Sertoli, Leydig, smooth muscle-like cells and various immune cells (Fig. 1C, E). Overall, >90% of cells in the atlas were differentiating germ cells, which is likely an overrepresentation of their relative abundances in intact tissue. We hypothesize that the enrichment of germ cells may be attributed to dissociation sensitivity, where irregular shape and large size of somatic cell types may have decreased their capture rate during 10X scRNAseq. Notably, every cluster is composed of cells from all four sample ages with the exception of cluster 14 which is unique to the 5 month atlas (Fig. S1E). Top differentially expressed genes in this cluster are associated with cell types found in the liver, suggesting this cluster is derived from contamination during dissection. We conclude that our composite atlas captures all known testis cell types and can serve as a cell type reference for this tissue. A web-based application for exploring the single-cell datasets presented in this paper is available at https://github.com/asposato/zebrafish_testis_fertility.

Testes from infertile zebrafish lack fully differentiated germ cells

A scRNAseq atlas of the infertile zebrafish testis would permit comparisons to uncover the mechanisms that regulate fertility. In laboratory settings, domesticated zebrafish can live for 3-5 years but fecundity decreases around 2 years of age. Testes of infertile animals are smaller and disorganized with expanded interstitial spaces and germ cells in less dense clusters (Fig. 2A, B). Representative images of infertile zebrafish demonstrate that the remaining germ cells within seminiferous tubules are mostly at earlier stages of spermatogenesis and interstitial spaces are expanded between tubules (Fig. S3). We dissected testes from two 27 month old zebrafish, dissociated whole tissue, and profiled each sample by scRNAseq. After filtering, the resulting infertile zebrafish testis atlas contained 24,469 cells (Fig. 2C, S4A).

We again identified all cell types within this atlas using marker genes (Fig. 2C, D, S4B). In the infertile atlas, only three clusters of germ cells were identified while the remaining 17 clusters were somatic cell types. While 93% of the cells in the composite fertile atlas are germ cells at various stages of development, germ cells make up only 32% of the infertile atlas. Of the germ cell clusters, marker genes for spermatogonia and spermatocytes are detected, yet post-meiotic germ cells were absent (Fig. 2D). Instead, somatic cell types make up the majority of the infertile atlas with immune cells accounting for much of this increase.

Somatic cell type composition shifts in the infertile testis

We compared somatic cell types between fertile and infertile testes to discover changes that may correlate with infertility. Coordination among immune cells is critical to the establishment and maintenance of tissue homeostasis (Bhushan et al. 2020, Fan et al. 2021). To investigate changes in immune cell composition, we subsetted immune cells from fertile and infertile testes using marker genes and reclustered these cells to create an immune atlas of the zebrafish testis (Fig. 3A, S5A). We identified cell types within this immune atlas using marker genes (Table 1, Fig. 3B, S5B). We found six T cell subtypes, natural killer cells, B cells, four macrophage subtypes, neutrophils, and one unknown leukocyte cell type. Most cells are from the infertile sample, although there was representation of all cell types within the fertile testes (Fig 3C, 5SA). We categorized cell types into broad somatic categories and calculated the relative abundance for each age. Many somatic cell types are elevated in infertile testes, particularly in macrophage and lymphocyte populations (Fig. 3D).

We also observed an expansion of some non-immune somatic cell populations in infertile testes (Fig. 3D). Split by cell type, blood cells and SMC-like cells were 9-fold higher in abundance in infertile testes, while Leydig and Sertoli cells proportionally decreased in abundance (Fig. 1E). Histological images (Fig. 1A-B, S2, 2A-B, S3) also show a large expansion of the interstitial spaces around tubules in infertile testes. To confirm changes in somatic cell abundances in the zebrafish testis, we used RNA in situ hybridization to detect macrophages and smooth muscle cells in both fertile and infertile testes. We found increased signal for the macrophage marker *mpeg1.1* and decreased signal for the smooth muscle marker *acta2* in infertile testes compared to fertile (Fig. 3E-F, S6A). Together, these data suggest that where germ cells are not progressing completely through spermatogenesis, the tubules give way to larger interstitial areas of connective tissue that contain many macrophages. Interestingly, while the proportion of blood and SMC-like cells seems to increase in infertile testes according to the single-cell data, molecular imaging shows that smooth muscle marker *acta2* diminishes in infertile testes. *Acta2* only weakly identifies SMC-like cells in the single-cell atlases. However, we do observe more abundant expression of *decorin* (*dcn*), a gene known to be expressed by stressed vascular endothelial cells and fibroblasts, in the SMC-like cells of the infertile testes (Fig. S6B, Järveläinen et al. 2015). The SMC-like cells in these interstitial areas may be breaking down between seminiferous tubules in aging testes.

Spermatogenesis is stable and continuous through fertility but incomplete in older testes

The absence of later stages of spermatogenesis in testes from infertile zebrafish led us to hypothesize that there may be a developmental block at meiosis. The difference in tissue integrity and lack of densely packed germ cells in the infertile histological images further supported this hypothesis (Fig. 1A-B, S2, 2A-B, S3). As animals age, we hypothesized that the proportion of germ cells may shift toward more spermatogonia compared to spermatozoa. 27 month-old testes completely lack spermatozoa but contain more spermatogonia than 5 month-old testes (Fig. 4A). Next, we sought to quantify how the progression of germ cell differentiation changed as the fertile testis ages using URD pseudotime analysis (Fig. 4B, Farrell et al. 2018). In this analysis, 0 represents the most spermatogonial state, and 1 represents the most differentiated spermatid state. We split the integrated object by age to visualize the proportion of germ cells at each stage of spermatogenesis (Fig. 4C). While all fertile stages were similar, we observed a modest increase in spermatogonial proportion and a

reciprocal decrease in contribution to later stages of spermatogenesis in older fertile testes (20 and 22 months) relative to testes from younger males (5 and 12 months). As animals approach infertility, our data suggests that the spermatogonia population declines in its ability to give rise to post-meiotic cells.

To investigate this phenomenon, we subsetted and reclustered spermatogonia from both fertile and infertile atlases. We found that the majority of germ cells from the infertile testes are transcriptionally distinct from fertile spermatogonia (Fig. 4D). Several known regulators of spermatogenesis such as *piwil1* and *ilf2* are more highly expressed in fertile germ cells compared to infertile (Fig. 4E). *E2f5,* recently identified as a new marker for undifferentiated spermatogonia (Xie et al. 2020, Qian et al. 2022), is highly expressed at 5 months, decreases in expression by 22 months, and is almost undetectable in spermatogonia from 27 month old testes. Perhaps the contrasting patterns of gene expression underlie the failure of spermatogonia in infertile testes to progress past meiosis. Together, our imaging and single-cell transcriptomic data suggest that infertile testes have a large population of spermatogonia and some spermatocytes but a dearth of post-meiotic cell types. We hypothesized that the expansion of immune cells we observe in infertile testes may help facilitate the apoptosis and removal of dying cells in the testis, perhaps explaining the absence of post-meiotic germ cells in infertile testes by a mechanism similar to what is observed in endocrine-disrupted testes (Haimbaugh et al. 2022). However, we did not detect differences in the expression of markers for apoptosis between fertile and infertile testes (Fig. S7), suggesting instead there may be a block at meiosis preventing the progression of germ cells past a critical checkpoint.

Discussion

In this study, we used timecourse scRNAseq to profile cells of the aging zebrafish testis. Our approach captures the stability of spermatogenesis during fertility and the dynamic changes within the testis during the onset of infertility. Germ cells are relatively stable in fertile zebrafish of all ages with proportions of germ cells following a consistent pattern across differentiation. In older yet still fertile testes, we observed a shift in abundance toward less differentiated cell types, but cell types at later stages of spermatogenesis are still detected. However, in infertile testes we did not detect post-meiotic germ cells. Histology of fertile and infertile testes confirmed that seminiferous tubules of fertile testes are densely packed with germ cells across the spectrum of differentiation while tubules of infertile testes have noticeably fewer germ cells of the size and density of post-meiotic germ cells. Infertile testes also exhibit reduced structural integrity with expanded interstitial spaces throughout the tissue without maintenance or expansion of smooth muscle. Infertile testes contain spermatogonial stem cells, but they have a distinct transcriptional identity and spermatogenesis is interrupted during or following the meiotic phase. Our developmental atlases describe testis composition across the fertile and infertile lifespan of a zebrafish, providing a foundation for probing the mechanisms underlying infertility.

Our results also highlight a diversity of immune cells lacking from previous scRNAseq studies of zebrafish testes. While some immune cells are found in the fertile atlas, the immune cell population of the infertile atlas is more diverse and proportionally far larger than the germ cell population. Notably, lymphocyte and macrophage populations form the majority of cells in infertile testes. In a previous study of endocrine disrupted testes, spermatogenesis failure in post-meiotic cells showed arrest or apoptosis of developing germ cells but does not characterize the immune cells of such tissues (Haimbaugh et al. 2022). In our data, it is unclear whether defects in meiosis or a post-meiotic event is responsible for the absence of these more differentiated cell types in naturally infertile testes. However, the increased presence of immune cells begs the question of whether immune cells act to inhibit fertility or, alternatively, whether they expand in older testes as a response to infertility. If immune cells prevent fertility, one might expect that immunosuppression could rescue fertility in

older animals that still contain spermatogonia. Alternatively, immune cells in older testes may regulate spermatogenesis to stave off production of defective sperm. Immune cells may arrive to clear out apoptosing germ cells that were rejected by cell autonomous or hormone-mediated quality control methods (Hikim et al. 2003). Tissue-specific perturbations to the testis immune cell population will be necessary to distinguish between these hypotheses and determine if the increased presence of immune cells in older fish is a cause or consequence of infertility.

Infertile zebrafish testes still contain early germ cells including spermatogonia. It would seem the stem cell pool is not depleted as male zebrafish age, but presence of these cells does not necessarily convey fertility. The spermatogonia population within the testis can be traced back to a small population of embryonic germ cells (Raz 2003). While the spermatogonia population that descends from these embryonic germ cells is maintained in the fertile testis for almost two years, perhaps the clonal diversity declines with age concomitant with the accumulation of detrimental mutations. Lineage tracing of the formation and maintenance of the spermatogonial population may uncover the mechanisms that direct clonality within the spermatogonial population and whether a decrease in clonal diversity accompanies infertility. We anticipate that transcriptomic resources, like those presented here, will facilitate continued explorations of the mechanisms that regulate the development, maintenance, and break down of the zebrafish testis and serve as an evolutionary comparison point for studies of fertility in other vertebrates (Green et al. 2018, Guo et al. 2018, Jung et al. 2019, Guo et al. 2020, Lau et al. 2020, Yu et al. 2021, Nie et al. 2022, Garcia-Alonso et al. 2022, Liu et al. 2022, Huang et al. 2023).

Methods

Zebrafish husbandry

All zebrafish used in this study were housed at the University of Utah CBRZ facility. This research was conducted under the approval of the Office of Institutional Animal Care and Use Committee (IACUC protocol 21-02017) of the University of Utah's animal care and use program.

Sample preparation and single-cell RNA sequencing

After euthanasia, testes were dissected and immediately placed in a dissociation solution of 440 µL 1X Hank's Balanced Salt Solution (HBSS), 50 µL 10% pluronic F-68, and 10 µL 0.26U/mL liberase TM. Tissue was incubated at 37°C for approximately 45 minutes while rotating at 750 rpm in an Eppendorf Thermomixer. The dissociation reaction was stopped by adding 1% bovine serum albumin (BSA) in 500 µL cold HBSS. The cell suspensions were filtered through a 40 µm cell strainer. Cells were pelleted in a 4°C centrifuge at 200g for 5 minutes, washed with 0.5% BSA in 500 µL cold HBSS, pelleted again and resuspended in 0.5% BSA in 500 µL cold HBSS. Single-cell RNA sequencing libraries were prepared by the University of Utah High-Throughput Genomics Shared Resource using the 10X Genomics Next GEM Single Cell 3' Gene Expression Library prep v3.1 with UDI. Libraries were sequenced with the NovaSeq Reagent Kit v1.5 150x150 bp Sequencing.

Data processing

Raw sequencing reads were processed by using 10X Genomics Cell Ranger software with the v4.3.2 transcriptome reference (Lawson et al. 2020). Further processing and cell clustering was conducted using Seurat v3 (Stuart et al. 2019). Log normalized gene expression was used for clustering of all atlases. To summarize, the barcode-feature matrices from Cell Ranger were converted to Seurat objects. Quality filtering steps included removing cells with >5% mitochondrial genes. Since rates of transcription in the testes are higher than any other organ, we used an interquartile range calculation to determine a reasonable range for

the number of genes per cell. We kept cells with >200 genes but fewer than *n* where *n* represents the largest value of the third quartile of each dataset. We used the integration function in Seurat v3 to integrate data sets which considered anchors determined by canonical correlation analysis. Analysis scripts, data, and a web-based app for exploration (Ouyang et al. 2021), are available at https://github.com/asposato/zebrafish_testis_fertility.

Trajectory analysis with URD

The fertile testis atlas Seurat object was converted to an URD object for pseudotime analysis (Farrell et al. 2018). We used the recommended knn of 199 (square root of total cell number). Each cell within the germ cell atlas was scored according to the state of differentiation. First, we assigned two clusters with the highest *ddx4* expression as the root cells (spermatogonia) and ran URD. Next, we assigned the cluster with the highest *tssk6* expression (spermatozoa) as the root cells and ran URD. We took the mean of the forward pseudotime and the inverse of the reverse pseudotime score to generate a spermatogenesis differentiation score for every germ cell.

Histology, RNAscope, and Imaging

Tissue for Hematoxylin and eosin (H&E) staining was processed using standard protocols (Siegfried and Steinfeld et al. 2021). Briefly, freshly dissected tissue was fixed in Davidsons' Fixative overnight at 4ºC. The tissue was then washed with 70% ethanol before processed for paraffin embedding. H&E staining was carried out on 5 µm thick tissue sections. Tissues used for RNAScope were fixed in 4% paraformaldehyde (PFA) overnight at 4ºC, sucrose treated, embedded in optimal cutting temperature compound (OCT), and cryosectioned into 7 µm thick sections. RNAscope® Multiplex Fluorescent Detection Kit v2 (Ref: 323110) and RNAScope probes for *mpeg1.1* (macrophages, Ref: 536171-C2) and *acta2* (vasculature, Ref: 508581-C3) were used as markers to identify cell types. Fluorescent images shown are maximum intensity projections that were tiled and stitched using ZEN Black software. Images of dissected testis tissue were taken with a Leica S9E stereo microscope. Histological images were captured with a Zeiss Axio Scan.Z1 Slide Scanner at 40X magnification. Fluorescent images were captured with a Zeiss 880 AiryScan confocal microscope.

Acknowledgements

We thank all members of the Gagnon lab for helpful discussions and comments. We thank Kellee Siegfried for help with the H&E staining protocol. We thank CZAR and CBRZ staff, especially Nathan Baker, for excellent zebrafish care. We thank the Cell Imaging, Genomics, and Histology core facilities. This project was supported by National Institutes of Health grants R35GM142950 (JAG), T32HD007491 (ALS), 1ZIAHD008997 (JAF), and T32GM141848 (JMW), by a University of Utah (U of U) College of Science Graduate Innovation Fellowship (ALS), by the Las Vegas Alumni Club Scholarship of the University of Utah Alumni Association (ALS), by the U of U Undergraduate Research Opportunity Program (DRL), by the U of U Summer Program for Undergraduate Research (HLH), and by startup funds from the Henry Eyring Center for Cell & Genome Science (JAG). This research was conducted on the traditional and ancestral homeland of the Shoshone, Paiute, Goshute, and Ute Tribes. We affirm and support the University of Utah's partnership with Native Nations and Urban Indian communities.

References

Beer, R.L., Draper, B.W., 2013. Nanos3 maintains germline stem cells and expression of the conserved germline stem cell gene nanos2 in the zebrafish ovary. Developmental Biology 374, 308–318. https://doi.org/10.1016/j.ydbio.2012.12.003

Bhushan, S., Theas, M.S., Guazzone, V.A., Jacobo, P., Wang, M., Fijak, M., Meinhardt, A., Lustig, L., 2020. Immune Cell Subtypes and Their Function in the Testis. Frontiers in Immunology 11.

Craig, M.P., Grajevskaja, V., Liao, H.-K., Balciuniene, J., Ekker, S.C., Park, J.-S., Essner, J.J., Balciunas, D., Sumanas, S., 2015. Etv2 and fli1b function together as key regulators of vasculogenesis and angiogenesis. Arterioscler Thromb Vasc Biol 35, 865–876. https://doi.org/10.1161/ATVBAHA.114.304768

Crespo, D., Assis, L.H.C., Zhang, Y.T., Safian, D., Furmanek, T., Skaftnesmo, K.O., Norberg, B., Ge, W., Choi, Y.-C., den Broeder, M.J., Legler, J., Bogerd, J., Schulz, R.W., 2021. Insulin-like 3 affects zebrafish spermatogenic cells directly and via Sertoli cells. Commun Biol 4, 1–13. https://doi.org/10.1038/s42003-021-01708-y

de Siqueira-Silva, D.H., da Silva Rodrigues, M., Nóbrega, R.H., 2019. Testis structure, spermatogonial niche and Sertoli cell efficiency in Neotropical fish. General and Comparative Endocrinology, Endocrinology of Neotropical Vertebrates 273, 218–226. https://doi.org/10.1016/j.ygcen.2018.09.004

Fan, X., Cui, L., Hou, T., Xue, X., Zhang, S., Wang, Z., 2021. Stress responses of testicular development, inflammatory and apoptotic activities in male zebrafish (Danio rerio) under starvation. Developmental & Comparative Immunology 114, 103833. https://doi.org/10.1016/j.dci.2020.103833

Farrell, J.A., Wang, Y., Riesenfeld, S.J., Shekhar, K., Regev, A., Schier, A.F., 2018. Single-cell reconstruction of developmental trajectories during zebrafish embryogenesis. Science 360, eaar3131. https://doi.org/10.1126/science.aar3131

Fritsch, M., Günther, S.D., Schwarzer, R., Albert, M.-C., Schorn, F., Werthenbach, J.P., Schiffmann, L.M., Stair, N., Stocks, H., Seeger, J.M., Lamkanfi, M., Krönke, M., Pasparakis, M., Kashkar, H., 2019. Caspase-8 is the molecular switch for apoptosis, necroptosis and pyroptosis. Nature 575, 683–687. https://doi.org/10.1038/s41586-019-1770-6

Garcia-Alonso, L., Lorenzi, V., Mazzeo, C.I., Alves-Lopes, J.P., Roberts, K., Sancho-Serra, C., Engelbert, J., Marečková, M., Gruhn, W.H., Botting, R.A., Li, T., Crespo, B., van Dongen, S., Kiselev, V.Y., Prigmore, E., Herbert, M., Moffett, A., Chédotal, A., Bayraktar, O.A., Surani, A., Haniffa, M., Vento-Tormo, R., 2022. Single-cell roadmap of human gonadal development. Nature 2022 607:7919 607, 540–547. https://doi.org/10.1038/s41586-022-04918-4

García-López, A., de Jonge, H., Nóbrega, R.H., de Waal, P.P., van Dijk, W., Hemrika, W., Taranger, G.L., Bogerd, J., Schulz, R.W., 2010. Studies in zebrafish reveal unusual cellular expression patterns of gonadotropin receptor messenger ribonucleic acids in the testis and unexpected functional differentiation of the gonadotropins. Endocrinology 151, 2349–2360. https://doi.org/10.1210/en.2009-1227

Gautier, A., Sohm, F., Joly, J.-S., Le Gac, F., Lareyre, J.-J., 2011. The Proximal Promoter Region of the Zebrafish gsdf Gene Is Sufficient to Mimic the Spatio-Temporal Expression Pattern of the Endogenous Gene in Sertoli and Granulosa Cells1. Biology of Reproduction 85, 1240–1251. https://doi.org/10.1095/biolreprod.111.091892

Georgijevic, S., Subramanian, Y., Rollins, E.-L., Starovic-Subota, O., Tang, A.C.Y., Childs, S.J., 2007. Spatiotemporal expression of smooth muscle markers in developing zebrafish gut. Developmental Dynamics 236, 1623–1632. https://doi.org/10.1002/dvdy.21165

Green, C.D., Ma, Q., Manske, G.L., Shami, A.N., Zheng, X., Marini, S., Moritz, L., Sultan, C., Gurczynski, S.J., Moore, B.B., Tallquist, M.D., Li, J.Z., Hammoud, S.S., 2018. A Comprehensive Roadmap of Murine Spermatogenesis Defined by Single-Cell RNA-Seq. Developmental cell 46, 651-667.e10. https://doi.org/10.1016/j.devcel.2018.07.025

Guo, J., Grow, E.J., Mlcochova, H., Maher, G.J., Lindskog, C., Nie, X., Guo, Y., Takei, Y., Yun, J., Cai, L., Kim, R., Carrell, D.T., Goriely, A., Hotaling, J.M., Cairns, B.R., 2018. The adult human testis transcriptional cell atlas. Cell Research 28, 1141–1157. https://doi.org/10.1038/s41422-018-0099-2

Guo, J., Nie, X., Giebler, M., Mlcochova, H., Wang, Y., Grow, E.J., Kim, R., Tharmalingam, M., Matilionyte, G., Lindskog, C., 2020. The dynamic transcriptional cell atlas of testis development during human puberty. Cell stem cell 26, 262–276.

Haimbaugh, A., Akemann, C., Meyer, D., Gurdziel, K., Baker, T.R., 2022. Insight into 2,3,7,8-tetrachlorodibenzo-p-dioxin-induced disruption of zebrafish spermatogenesis via single cell RNA-seq. PNAS Nexus 1, pgac060. https://doi.org/10.1093/pnasnexus/pgac060

Hambarde, S., Tsai, C.-L., Pandita, R.K., Bacolla, A., Maitra, A., Charaka, V., Hunt, C.R., Kumar, R., Limbo, O., Le Meur, R., Chazin, W.J., Tsutakawa, S., Russell, P., Schlacher, K., Pandita, T.K., Tainer, J.A., 2021. EXO5-DNA Structure and BLM Interactions Direct DNA Resection Critical for ATR-dependent Replication Restart. Mol Cell 81, 2989-3006.e9. https://doi.org/10.1016/j.molcel.2021.05.027

Haupt, Y., Barak, Y., Oren, M., 1996. Cell type-specific inhibition of p53-mediated apoptosis by mdm2. The EMBO Journal 15, 1596–1606. https://doi.org/10.1002/j.1460-2075.1996.tb00504.x

Hikim, A.P.S., Lue, Y., Yamamoto, C.M., Vera, Y., Rodriguez, S., Yen, P.H., Soeng, K., Wang, C., Swerdloff, R.S., 2003. Key Apoptotic Pathways for Heat-Induced Programmed Germ Cell Death in the Testis. Endocrinology 144, 3167–3175. https://doi.org/10.1210/en.2003-0175

Houwing, S., Kamminga, L.M., Berezikov, E., Cronembold, D., Girard, A., van den Elst, H., Filippov, D.V., Blaser, H., Raz, E., Moens, C.B., Plasterk, R.H.A., Hannon, G.J., Draper, B.W., Ketting, R.F., 2007. A Role for Piwi and piRNAs in Germ Cell Maintenance and Transposon Silencing in Zebrafish. Cell 129, 69–82. https://doi.org/10.1016/J.CELL.2007.03.026

Huang, L., Zhang, J., Zhang, P., Huang, X., Yang, W., Liu, R., Sun, Q., Lu, Y., Zhang, M., Fu, Q., 2023. Single-cell RNA sequencing uncovers dynamic roadmap and cell-cell communication during buffalo spermatogenesis. iScience 26, 105733. https://doi.org/10.1016/j.isci.2022.105733

Järveläinen, H., Sainio, A., Wight, T.N., 2015. Pivotal role for decorin in angiogenesis. Matrix Biology 43, 15–26. https://doi.org/10.1016/j.matbio.2015.01.023

Kalev-Zylinska, M.L., Horsfield, J.A., Flores, M.V.C., Postlethwait, J.H., Chau, J.Y.M., Cattin, P.M., Vitas, M.R., Crosier, P.S., Crosier, K.E., 2003. Runx3 is required for hematopoietic development in zebrafish. Developmental Dynamics 228, 323–336. https://doi.org/10.1002/dvdy.10388

Kuil, L.E., Oosterhof, N., Ferrero, G., Mikulášová, T., Hason, M., Dekker, J., Rovira, M., van der Linde, H.C., van Strien, P.M., de Pater, E., Schaaf, G., Bindels, E.M., Wittamer, V., van Ham, T.J., 2020. Zebrafish macrophage developmental arrest underlies depletion of microglia and reveals Csf1r-independent metaphocytes. eLife 9, e53403. https://doi.org/10.7554/eLife.53403

Lau, X., Munusamy, P., Ng, M.J., Sangrithi, M., 2020. Single-Cell RNA Sequencing of the Cynomolgus Macaque Testis Reveals Conserved Transcriptional Profiles during Mammalian Spermatogenesis. Developmental Cell 54, 548-566.e7. https://doi.org/10.1016/j.devcel.2020.07.018

Lawson, N.D., Li, R., Shin, M., Grosse, A., Onur, Y.M.S., Stone, O.A., Kucukural, A., Zhu, L.J., 2020. An improved zebrafish transcriptome annotation for sensitive and comprehensive detection of cell type-specific genes. eLife 9, 1–76. https://doi.org/10.7554/ELIFE.55792

Leal, M.C., Cardoso, E.R., Nó, R.H., Batlouni, S.R., Bogerd, J., França, L.R., Diger, R., Schulz, W., 2009. Histological and Stereological Evaluation of Zebrafish (Danio rerio) Spermatogenesis with an Emphasis on Spermatogonial Generations 1. BIOLOGY OF REPRODUCTION 81, 177–187. https://doi.org/10.1095/biolreprod.109.076299

Lee, S.L.J., Horsfield, J.A., Black, M.A., Rutherford, K., Fisher, A., Gemmell, N.J., 2017. Histological and transcriptomic effects of 17α-methyltestosterone on zebrafish gonad development. BMC Genomics 18, 557. https://doi.org/10.1186/s12864-017-3915-z

Li, X., Zhang, F., Wu, N., Ye, D., Wang, Y., Zhang, X., Sun, Y., Zhang, Y.-A., 2020. A critical role of foxp3a-positive regulatory T cells in maintaining immune homeostasis in zebrafish testis development. Journal of Genetics and Genomics 47, 547–561. https://doi.org/10.1016/j.jgg.2020.07.006

Li, Y., Sosnik, J., Brassard, L., Reese, M., Spiridonov, N.A., Bates, T.C., Johnson, G.R., Anguita, J., Visconti, P.E., Salicioni, A.M., 2011. Expression and localization of five members of the testis-specific serine kinase (Tssk) family in mouse and human sperm and testis. Mol Hum Reprod 17, 42–56. https://doi.org/10.1093/molehr/gaq071

Liu, Y., Kossack, M.E., McFaul, M.E., Christensen, L.N., Siebert, S., Wyatt, S.R., Kamei, C.N., Horst, S., Arroyo, N., Drummond, I.A., 2022. Single-cell transcriptome reveals insights into the development and function of the zebrafish ovary. Elife 11, e76014.

Maack, G., Segner, H., 2003. Morphological development of the gonads in zebrafish. Journal of Fish Biology 62, 895–906. https://doi.org/10.1046/j.1095-8649.2003.00074.x

Mathias, J.R., Perrin, B.J., Liu, T.-X., Kanki, J., Look, A.T., Huttenlocher, A., 2006. Resolution of inflammation by retrograde chemotaxis of neutrophils in transgenic zebrafish. J Leukoc Biol 80, 1281–1288. https://doi.org/10.1189/jlb.0506346

Matzkin, M.E., Miquet, J.G., Fang, Y., Hill, C.M., Turyn, D., Calandra, R.S., Bartke, A., Frungieri, M.B., 2016. Alterations in oxidative, inflammatory and apoptotic events in short-lived and long-lived mice testes. Aging (Albany NY) 8, 95–110.

Meijer, A.H., van der Sar, A.M., Cunha, C., Lamers, G.E.M., Laplante, M.A., Kikuta, H., Bitter, W., Becker, T.S., Spaink, H.P., 2008. Identification and real-time imaging of a myc-expressing neutrophil population involved in inflammation and mycobacterial granuloma formation in zebrafish. Dev Comp Immunol 32, 36–49. https://doi.org/10.1016/j.dci.2007.04.003

Melé, M., Ferreira, P.G., Reverter, F., DeLuca, D.S., Monlong, J., Sammeth, M., Young, T.R., Goldmann, J.M., Pervouchine, D.D., Sullivan, T.J., Johnson, R., Segrè, A.V., Djebali, S., Niarchou, A., Consortium, T.Gte., Wright, F.A., Lappalainen, T., Calvo, M., Getz, G., Dermitzakis, E.T., Ardlie, K.G., Guigó, R., 2015. The human transcriptome across tissues and individuals. Science 348, 660–665. https://doi.org/10.1126/science.aaa0355

Nie, X., Munyoki, S.K., Sukhwani, M., Schmid, N., Missel, A., Emery, B.R., DonorConnect, Stukenborg, J.-B., Mayerhofer, A., Orwig, K.E., Aston, K.I., Hotaling, J.M., Cairns, B.R., Guo, J., 2022. Single-cell analysis of human testis aging and correlation with elevated body mass index. Developmental Cell 57, 1160-1176.e5. https://doi.org/10.1016/j.devcel.2022.04.004

Ouyang, J.F., Kamaraj, U.S., Cao, E.Y., Rackham, O.J.L., 2021. ShinyCell: simple and sharable visualization of single-cell gene expression data. Bioinformatics 37, 3374–3376. https://doi.org/10.1093/bioinformatics/btab209

Ozaki, Y., Saito, K., Shinya, M., Kawasaki, T., Sakai, N., 2011. Evaluation of Sycp3, Plzf and cyclin B3 expression and suitability as spermatogonia and spermatocyte markers in zebrafish. Gene Expression Patterns 11, 309–315. https://doi.org/10.1016/j.gep.2011.03.002

Pereiro, P., Varela, M., Diaz-Rosales, P., Romero, A., Dios, S., Figueras, A., Novoa, B., 2015. Zebrafish Nk-lysins: First insights about their cellular and functional diversification. Developmental & Comparative Immunology 51, 148–159. https://doi.org/10.1016/j.dci.2015.03.009

Qian, P., Kang, J., Liu, D., Xie, G., 2022. Single Cell Transcriptome Sequencing of Zebrafish Testis Revealed Novel Spermatogenesis Marker Genes and Stronger Leydig-Germ Cell Paracrine Interactions. Frontiers in Genetics 13.

Raz, E., 2003. Primordial germ-cell development: the zebrafish perspective. Nature Reviews Genetics 4, 690–700. https://doi.org/10.1038/nrg1154

Roessler, S., Györy, I., Imhof, S., Spivakov, M., Williams, R.R., Busslinger, M., Fisher, A.G., Grosschedl, R., 2007. Distinct promoters mediate the regulation of Ebf1 gene expression by interleukin-7 and Pax5. Mol Cell Biol 27, 579–594. https://doi.org/10.1128/MCB.01192-06

Rougeot, J., Torraca, V., Zakrzewska, A., Kanwal, Z., Jansen, H.J., Sommer, F., Spaink, H.P., Meijer, A.H., 2019. RNAseq Profiling of Leukocyte Populations in Zebrafish Larvae Reveals a cxcl11 Chemokine Gene as a Marker of Macrophage Polarization During Mycobacterial Infection. Frontiers in Immunology 10.

Santoro, M.M., Pesce, G., Stainier, D.Y., 2009. Characterization of vascular mural cells during zebrafish development. Mech Dev 126, 638–649. https://doi.org/10.1016/j.mod.2009.06.1080

Schulz, R.W., de França, L.R., Lareyre, J.-J., LeGac, F., Chiarini-Garcia, H., Nobrega, R.H., Miura, T., 2010. Spermatogenesis in fish. General and Comparative Endocrinology, Fish Reproduction 165, 390–411. https://doi.org/10.1016/j.ygcen.2009.02.013

Schulz, R.W., Menting, S., Bogerd, J., França, L.R., Vilela, D.A.R., Godinho, H.P., 2005. Sertoli Cell Proliferation in the Adult Testis—Evidence from Two Fish Species Belonging to Different Orders1. Biology of Reproduction 73, 891–898. https://doi.org/10.1095/biolreprod.105.039891

Siegfried, K.R., Steinfeld, J.S., 2021. Histological analysis of gonads in zebrafish. Germline Development in the Zebrafish: Methods and Protocols 253–263.

Song, H.-D., Sun, X.-J., Deng, M., Zhang, G.-W., Zhou, Y., Wu, X.-Y., Sheng, Y., Chen, Y., Ruan, Z., Jiang, C.-L., Fan, H.-Y., Zon, L.I., Kanki, J.P., Liu, T.X., Look, A.T., Chen, Z., 2004. Hematopoietic gene expression profile in zebrafish kidney marrow. Proceedings of the National Academy of Sciences 101, 16240–16245. https://doi.org/10.1073/pnas.0407241101

Soumillon, M., Necsulea, A., Weier, M., Brawand, D., Zhang, X., Gu, H., Barthes, P., Kokkinaki, M., Nef, S., Gnirke, A., 2013. Cellular source and mechanisms of high transcriptome complexity in the mammalian testis. Cell reports 3, 2179–2190.

Stuart, T., Butler, A., Hoffman, P., Hafemeister, C., Papalexi, E., Mauck, W.M., Hao, Y., Stoeckius, M., Smibert, P., Satija, R., 2019. Comprehensive Integration of Single-Cell Data. Cell 177, 1888-1902.e21. https://doi.org/10.1016/j.cell.2019.05.031

Tomasini, R., Seux, M., Nowak, J., Bontemps, C., Carrier, A., Dagorn, J.-C., Pébusque, M.-J., Iovanna, J.L., Dusetti, N.J., 2005. TP53INP1 is a novel p73 target gene that induces cell cycle arrest and cell death by modulating p73 transcriptional activity. Oncogene 24, 8093–8104. https://doi.org/10.1038/sj.onc.1208951

Uribe, M.C., Grier, H.J., Mejía-Roa, V., 2014. Comparative testicular structure and spermatogenesis in bony fishes. Spermatogenesis 4, e983400. https://doi.org/10.4161/21565562.2014.983400

Walker, W.H., 2010. Non-classical actions of testosterone and spermatogenesis. Philos Trans R Soc Lond B Biol Sci 365, 1557–1569. https://doi.org/10.1098/rstb.2009.0258

Wang, X.G., Bartfai, R., Sleptsova-Freidrich, I., Orban, L., 2007. The timing and extent of 'juvenile ovary' phase are highly variable during zebrafish testis differentiation. Journal of Fish Biology 70, 33–44. https://doi.org/10.1111/j.1095-8649.2007.01363.x

Webster, K.A., Schach, U., Ordaz, A., Steinfeld, J.S., Draper, B.W., Siegfried, K.R., 2017. Dmrt1 is necessary for male sexual development in zebrafish. Developmental Biology 422, 33–46. https://doi.org/10.1016/j.ydbio.2016.12.008

Wu, H., Chen, Y., Miao, S., Zhang, C., Zong, S., Koide, S.S., Wang, L., 2010. Sperm associated antigen 8 (SPAG8), a novel regulator of activator of CREM in testis during spermatogenesis. FEBS Letters 584, 2807–2815. https://doi.org/10.1016/j.febslet.2010.05.016

Xia, B., Yan, Y., Baron, M., Wagner, F., Barkley, D., Chiodin, M., Kim, S.Y., Keefe, D.L., Alukal, J.P., Boeke, J.D., Yanai, I., 2020. Widespread Transcriptional Scanning in the Testis Modulates Gene Evolution Rates. Cell 180, 248-262.e21. https://doi.org/10.1016/j.cell.2019.12.015

Xie, H., Kang, Y., Wang, S., Zheng, P., Chen, Z., Roy, S., Zhao, C., 2020. E2f5 is a versatile transcriptional activator required for spermatogenesis and multiciliated cell differentiation in zebrafish. PLOS Genetics 16, e1008655–e1008655. https://doi.org/10.1371/JOURNAL.PGEN.1008655

Ye, D., Liu, T., Li, Y., Wang, Y., Hu, W., Zhu, Z., Sun, Y., 2023. Identification of fish spermatogenic cells through high-throughput immunofluorescence against testis with an antibody set. Frontiers in Endocrinology 14, 1–14. https://doi.org/10.3389/fendo.2023.1044318

Yoon, C., Kawakami, K., Hopkins, N., 1997. Zebrafish vasa homologue RNA is localized to the cleavage planes of 2- and 4-cell-stage embryos and is expressed in the primordial germ cells. Development 124, 3157–3165. https://doi.org/10.1242/dev.124.16.3157

Yoon, S., Mitra, S., Wyse, C., Alnabulsi, A., Zou, J., Weerdenburg, E.M., Sar, A.M. van der, Wang, D., Secombes, C.J., Bird, S., 2015. First Demonstration of Antigen Induced Cytokine Expression by CD4-1+ Lymphocytes in a Poikilotherm: Studies in Zebrafish (Danio rerio). PLOS ONE 10, e0126378. https://doi.org/10.1371/journal.pone.0126378

Yu, X.-W., Li, T.-T., Du, X.-M., Shen, Q.-Y., Zhang, M.-F., Wei, Y.-D., Yang, D.-H., Xu, W.-J., Chen, W.-B., Bai, C.-L., Li, X.-L., Li, G.-P., Li, N., Peng, S., Liao, M.-Z., Hua, J.-L., 2021. Single-cell RNA sequencing reveals atlas of dairy goat testis cells. Zool Res 42, 401–405. https://doi.org/10.24272/j.issn.2095-8137.2020.373

Zhang, X., Tang, N., Hadden, T.J., Rishi, A.K., 2011. Akt, FoxO and regulation of apoptosis. Biochim Biophys Acta 1813, 1978–1986. https://doi.org/10.1016/j.bbamcr.2011.03.010

Zhang, Y., Li, Z., Nie, Y., Ou, G., Chen, C., Cai, S., Liu, L., Yang, P., 2020. Sexually dimorphic reproductive defects in zebrafish with spo11 mutation. Aquaculture Research 51, 4916–4924. https://doi.org/10.1111/are.14829

Figures

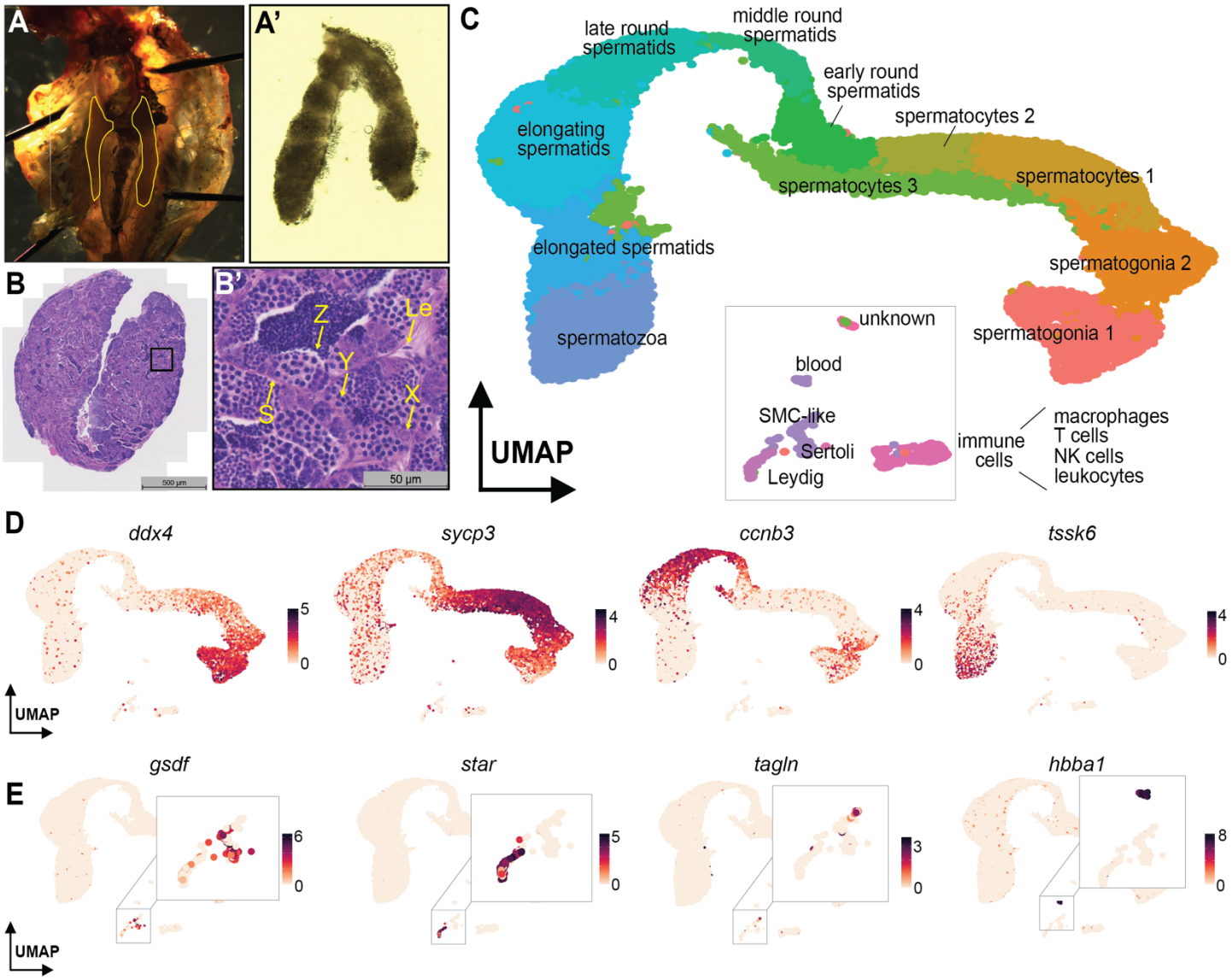

Figure 1. Single-cell RNA sequencing of 32,659 cells from six fertile adult zebrafish testes. **(A-A')** Testes dissected from fertile 12 month old zebrafish. Testes are highlighted in yellow in the trunk image (A). **(B-B')** Histology of adult testes from a 12 month old zebrafish. Yellow arrows point to basement membrane of seminiferous tubule (S), undifferentiated spermatogonia (X), spermatocytes (Y), spermatids (Z), and Leydig cell (Le). **(C)** An atlas of fertile zebrafish testes. Cell clusters were identified using canonical markers. **(D)** Representative markers of spermatogonia, spermatocytes, spermatids and spermatozoa. **(E)** Representative markers of Sertoli, Leydig, smooth muscle cells, and blood.

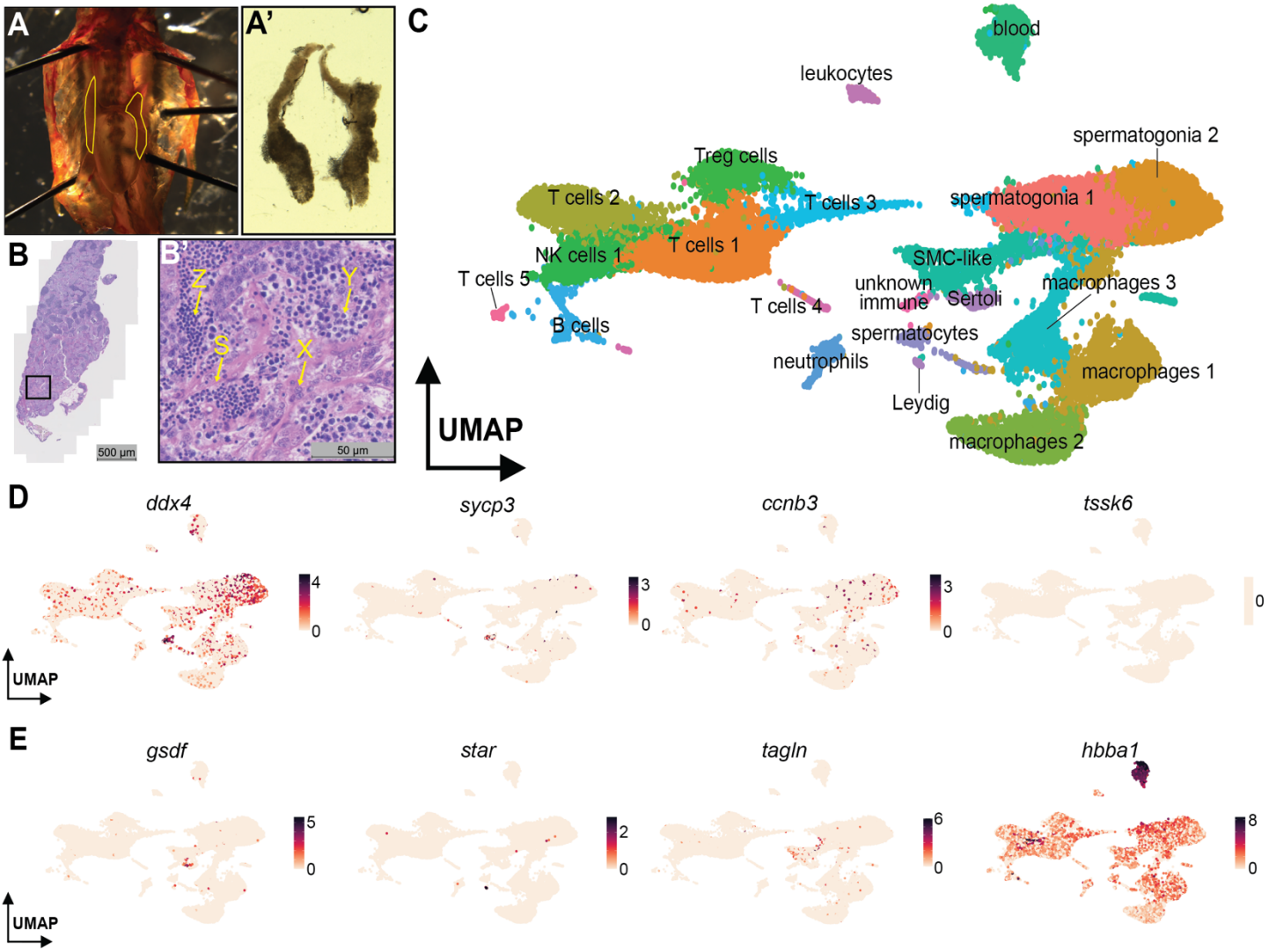

Figure 2. Single-cell RNA sequencing of 24,469 cells from two infertile 27 month old adult zebrafish testes. **(A-A')** Testes dissected from infertile 26 month old zebrafish. Testes are highlighted in yellow in the trunk image. **(B-B')** Histology of adult testes from a 26 month old zebrafish. Yellow arrows point to basement membrane of seminiferous tubule (S), undifferentiated spermatogonia (X), spermatocytes (Y) and spermatids (Z). **(C)** An atlas of infertile zebrafish testes. Cell clusters were identified using canonical markers. **(D)** Representative markers of spermatogonia and spermatocytes. Cyclin B3 (*ccnb3*) is expressed by round spermatids and 16-cell stage spermatogonial cysts. **(E)** Representative markers of Sertoli, Leydig, smooth muscle cells, and blood.

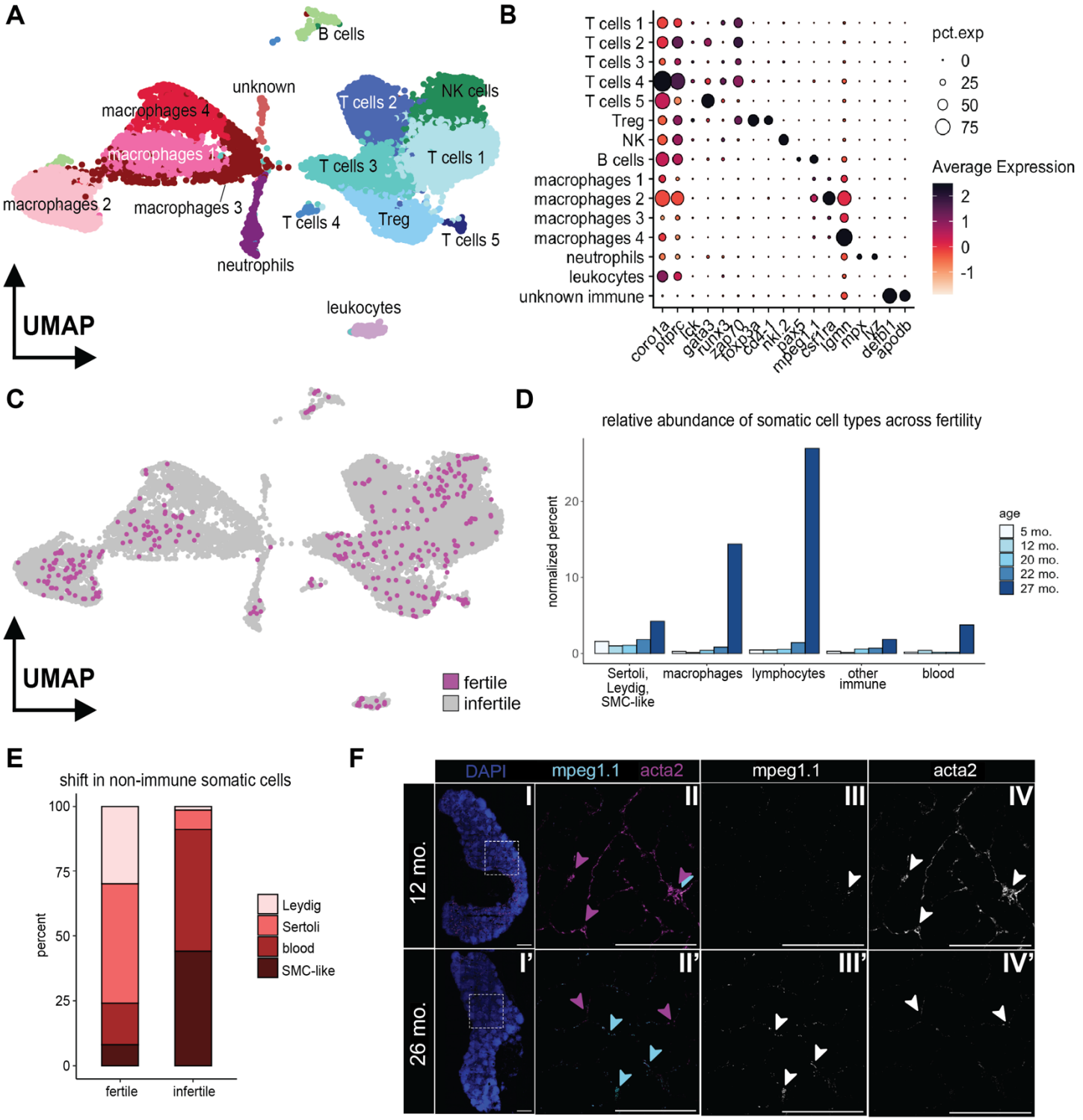

Figure 3. Reclustered immune cells from fertile and infertile atlases. **(A)** The infertile testes are enriched for immune cells. Particularly, large populations of T cells and macrophages were detected. **(B)** Canonical marker genes were used to identify each cell type. **(C)** Cells from fertile animals highlighted on immune cells atlas. **(D)** Relative abundance of somatic cell types from each sample age. **(E)** Proportions of Sertoli, Leydig, blood and smooth muscle in fertile and infertile testes. **(F)** RNAscope of smooth muscle marker *acta2* and macrophage marker *mpeg1.1* in fertile and infertile testes. (I-I') DAPI staining of testis lobes from 12 mo. and 26 mo. zebrafish. Square inset used for images in panels II-IV. (I-II') Merge of *acta2* (magenta) and *mpeg1.1* (cyan) markers. (III-III') Macrophage marker *mpeg1.1*. (IV-IV') Smooth muscle marker *acta2*. Arrowheads highlight examples of fluorescence.

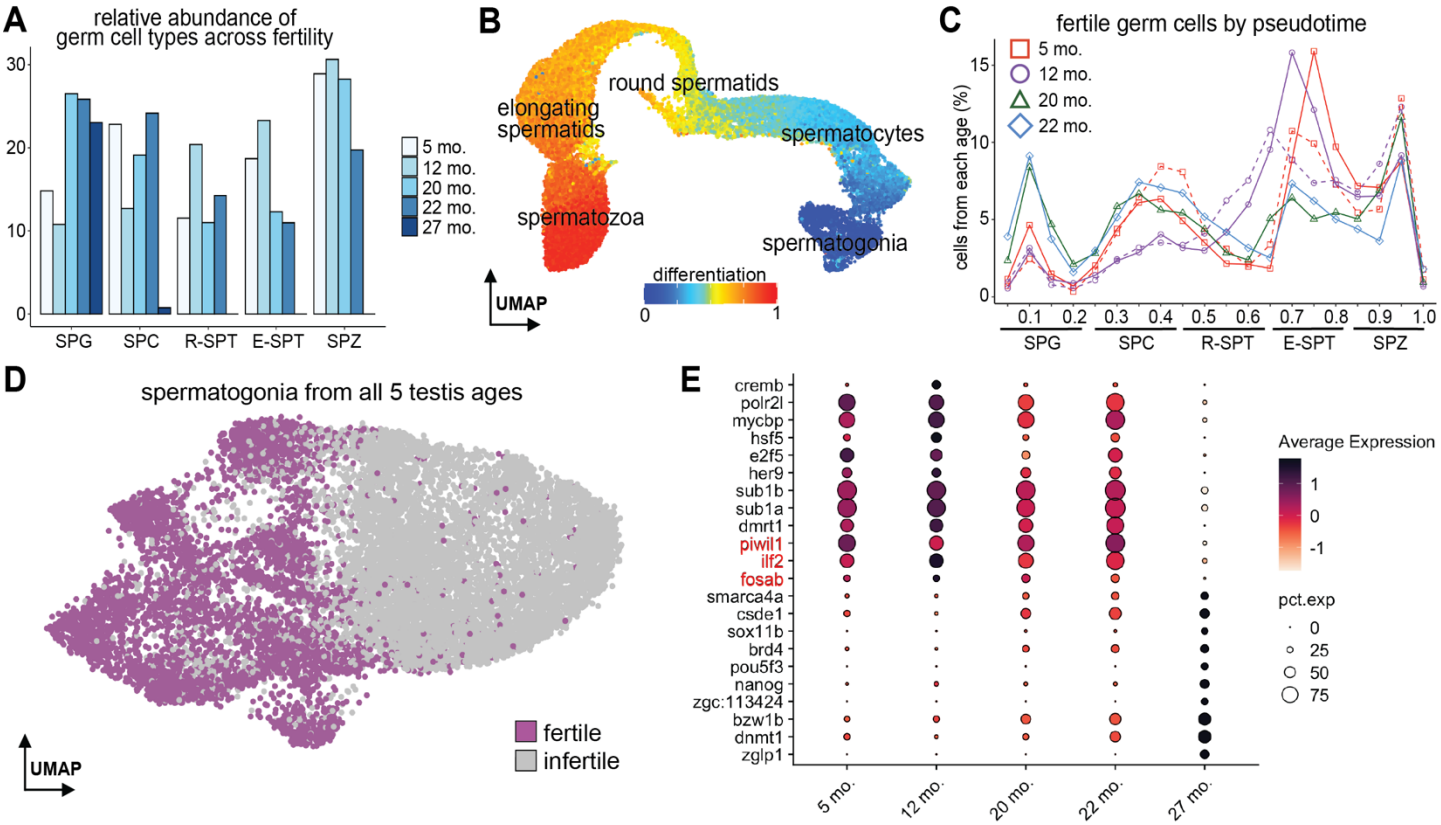

Figure 4. Spermatogenesis is stable and continuous through fertility.
(A) Relative abundance of germ cell types from each sample age. **(B)** Fertile germ cells colored by pseudotime-determined scores of differentiation using URD. **(C)** Normalized percent of cells from each fertile age binned across differentiation. Ages with replicates are denoted with dashed lines. **(D)** Reclustered spermatogonia from fertile and infertile atlases. **(E)** Dotplot shows the top 10 transcription factors for fertile and infertile testes compared with known regulators (emphasized in red).

cell type	marker	reference	DOI
germ cells	*ddx4*	Yoon et al., 1997	10.1242/dev.124.16.3157
	piwil1	Houwing et al., 2007	10.1016/j.cell.2007.03.026
	dmrt1	Webster et al., 2017	10.1016/j.ydbio.2016.12.008
spermatogonia	*sumo3b*	Qian et al., 2022	10.3389/fgene.2022.851719
	pcna	Ye et al., 2023	10.3389/fendo.2023.1044318
	hist1h4l	Qian et al., 2022	10.3389/fgene.2022.851719
	ccnb3	Ozaki et al., 2011	10.1016/j.gep.2011.03.002
spermatocytes	*sycp3*	Ozaki et al., 2011	10.1016/j.gep.2011.03.002
	dmc1	Beer & Draper, 2012	10.1016/j.ydbio.2012.12.003
	spo11	Zhang et al., 2020	10.1111/are.14829
	e2f5	Xie et al., 2020	10.1371/journal.pgen.1008655
spermatids	*ccnb3*	Ozaki et al., 2011	10.1016/j.gep.2011.03.002
	larp1b	Qian et al., 2022	10.3389/fgene.2022.851719
	edrf1	Qian et al., 2022	10.3389/fgene.2022.851719
spermatozoa	*tssk6*	Li. et al., 2011	10.1093/molehr/gaq071
	spag8	Wu et al., 2010	10.1016/j.febslet.2010.05.016
Sertoli	*gsdf*	Gautier et al., 2011	10.1095/biolreprod.111.091892
	krt18a.1	Qian et al., 2022	10.3389/fgene.2022.851719
Leydig	*star*	Gautier et al., 2011	10.1095/biolreprod.111.091892
	cyp17a2	Gautier et al., 2011	10.1095/biolreprod.111.091892
SMC-like	*tagln*	Santoro et al., 2009	10.1016/j.mod.2009.06.1080
	acta2	Georgijevic et al., 2007	10.1002/dvdy.21165
	dcn	Järveläinen et al., 2015	10.1016/j.matbio.2015.01.023
blood	*hbba1*	Qian et al., 2022	10.3389/fgene.2022.851719
	fli1b	Craig et al. 2015	10.1161/ATVBAHA.114.304768
leukocytes	*coro1a*	Song et al., 2004	10.1073/pnas.0407241101
	ptprc	Rougeot et al., 2019	10.3389/fimmu.2019.00832
macrophages	*mpeg1.1*	Kuil et al., 2020	10.7554/eLife.53403
	csf1ra	Kuil et al., 2020	10.7554/eLife.53403
T cells	*zap70*	Yoon et al., 2015	10.1371/journal.pone.0126378
	cd4-1	Yoon et al., 2015	10.1371/journal.pone.0126378
	runx3	Kalev-Zylinkska et al., 2003	10.1002/dvdy.10388
	foxp3a	Li. et al., 2020	10.1016/j.jgg.2020.07.006
neutrophils	*mpx*	Mathias et al., 2006	10.1189/jlb.0506346
	lyz	Meijer et al., 2007	10.1016/j.dci.2007.04.003
B cells	*pax5*	Roessler et al., 2007	10.1128/MCB.01192-06
NK cells	*nkl.2*	Pereiro et al., 2015	10.1016/j.dci.2015.03.009

562 **Table 1.** A subset of marker genes used to identify testicular cell types.
563
564

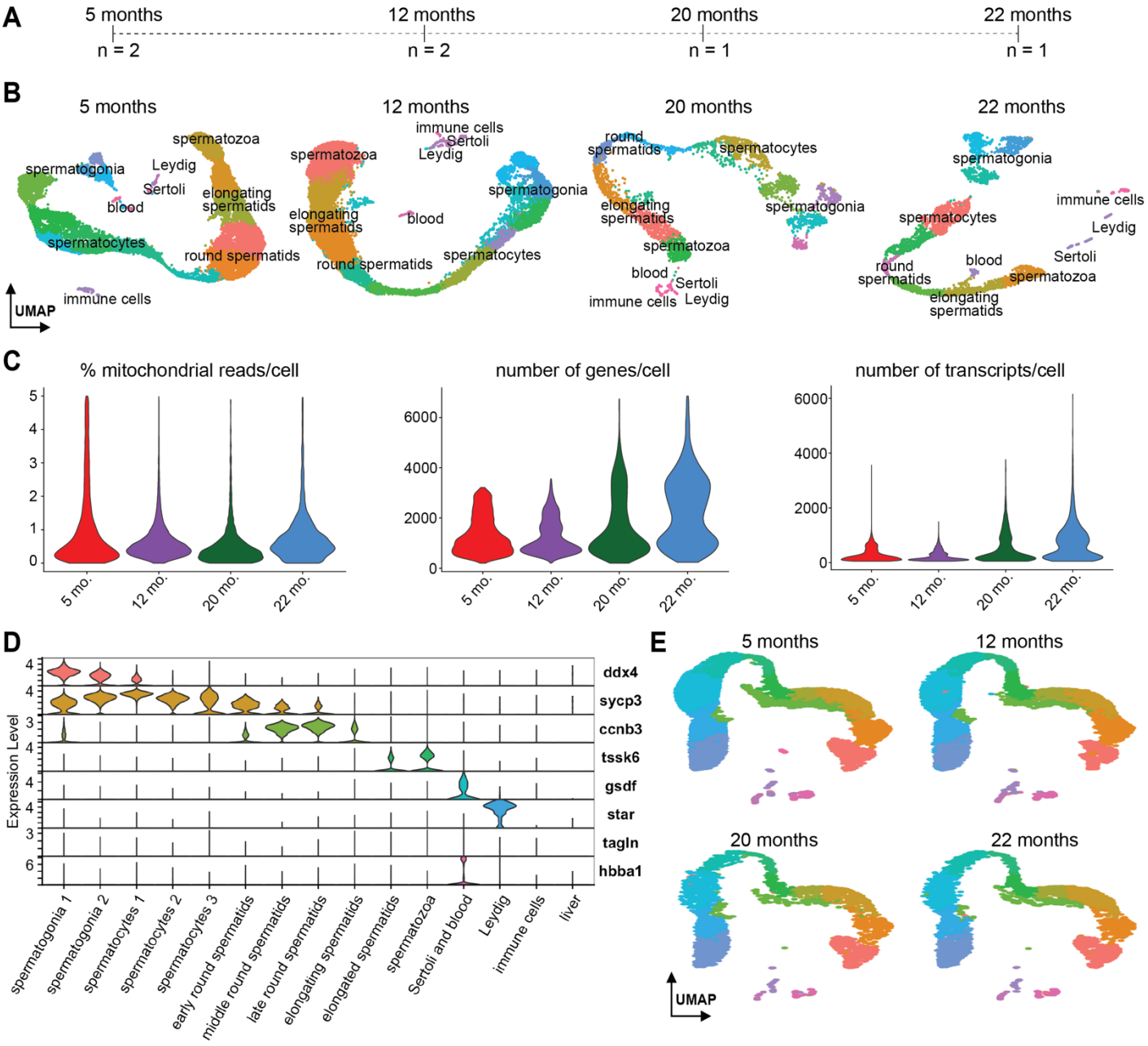

Supplemental Figure 1. Fertile atlas.
(A) Ages and sample sizes of testes comprising fertile atlas. **(B)** Individual UMAPs of each age comprising the fertile atlas. **(C)** Violin plots show the percent mitochondrial reads, number of genes, and number of transcripts per cell. **(D)** Violin plots of the marker genes used in Figure 1D-E. **(E)** Fertile atlas split by sample age.

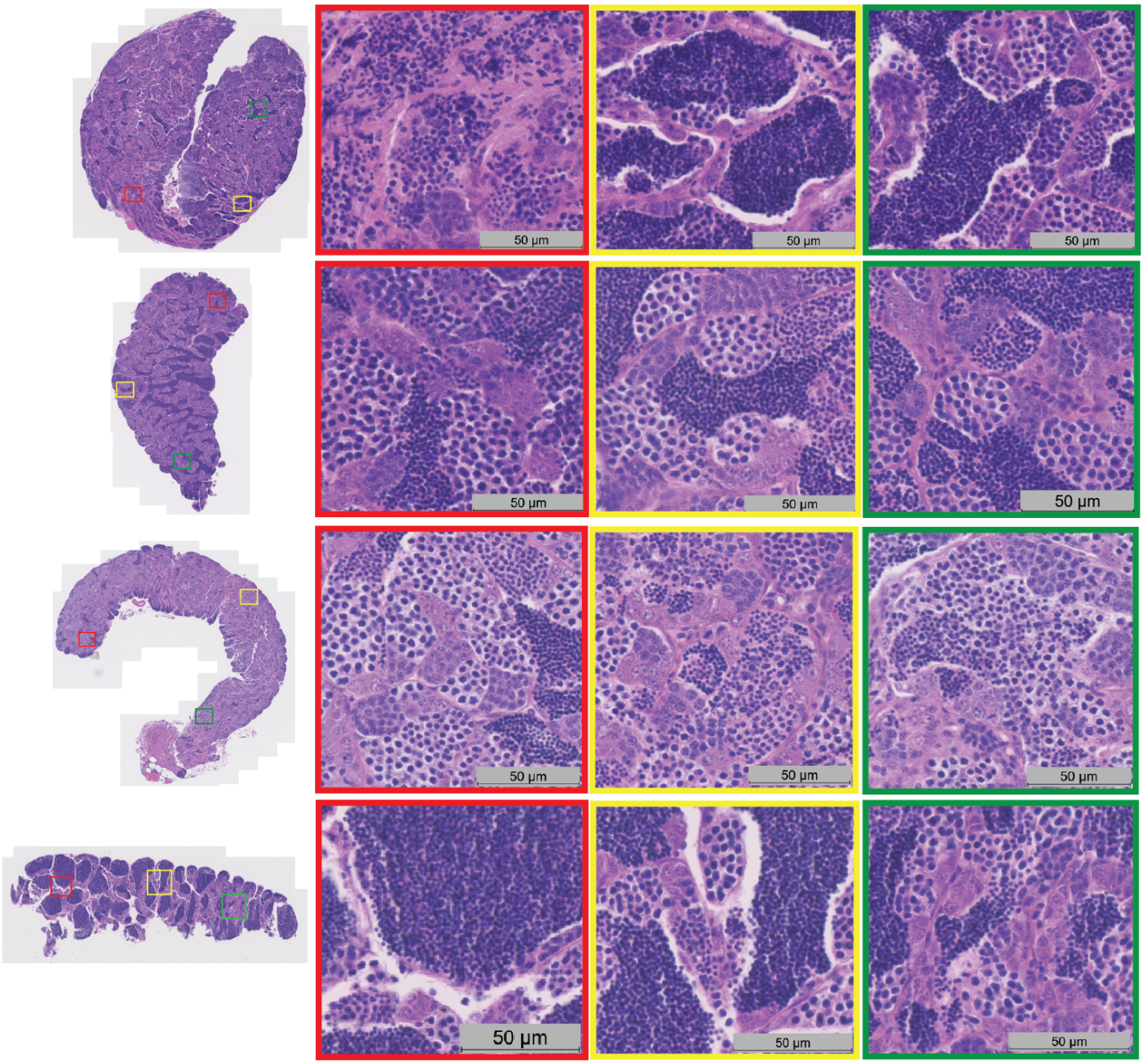

Supplemental Figure 2. Histology of fertile zebrafish testes.

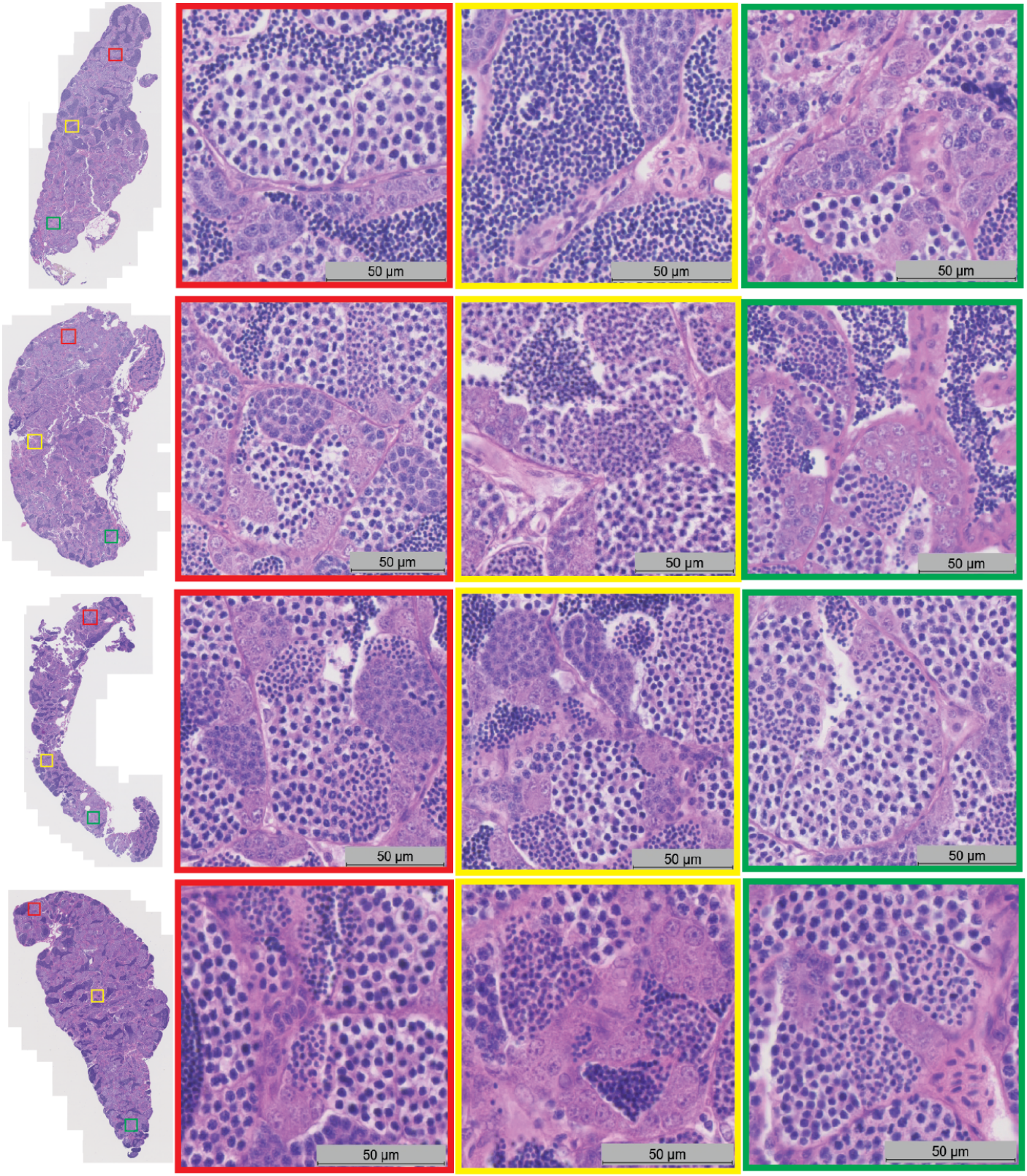

Supplemental Figure 3. Histology of infertile zebrafish testes.

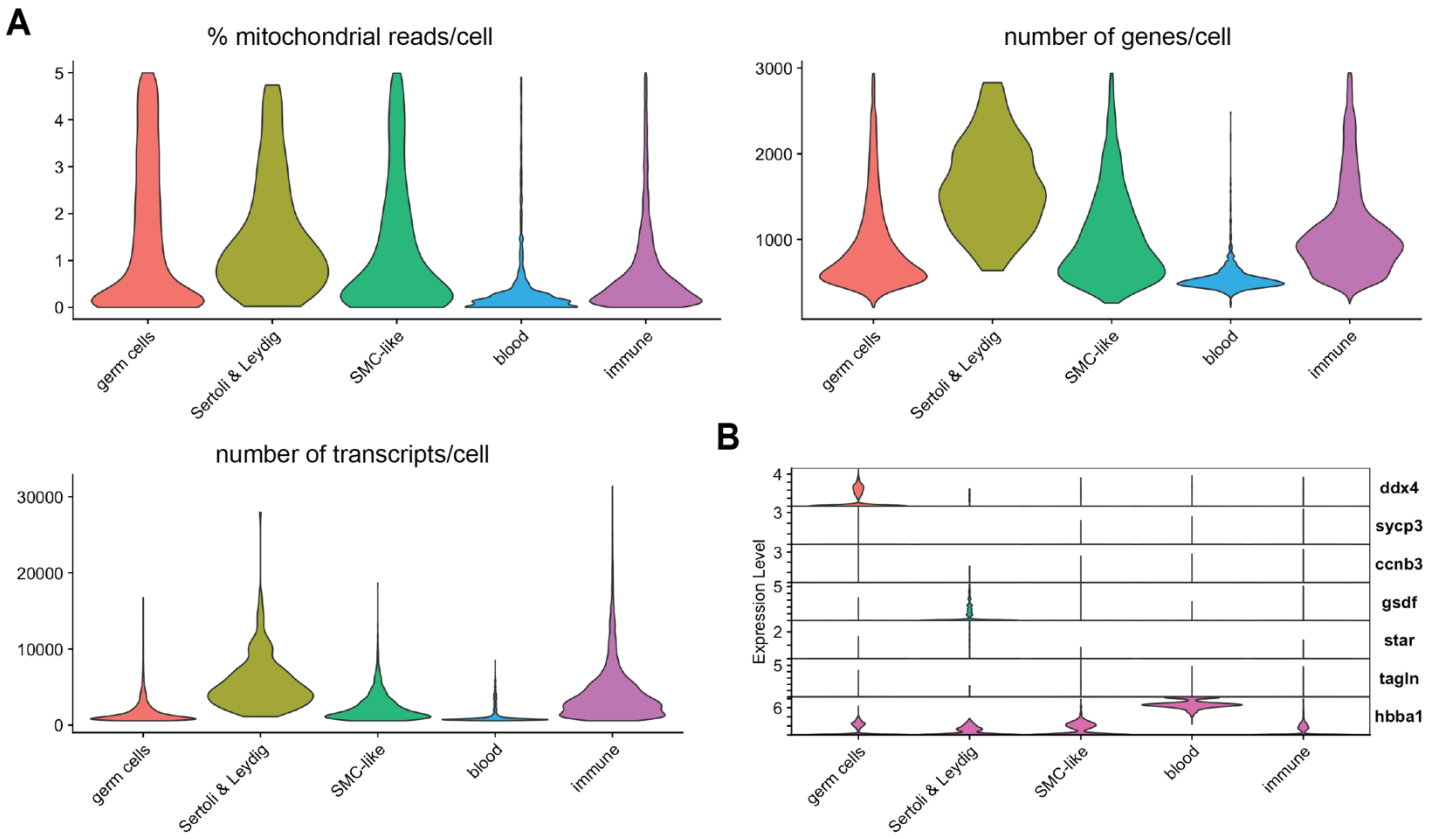

Supplemental Figure 4. Infertile atlas.
(A) Violin plots show the percent mitochondrial reads, number of genes, and number of transcripts per cell. **(B)** Violin plots of the marker genes used in Figure 2D-E.

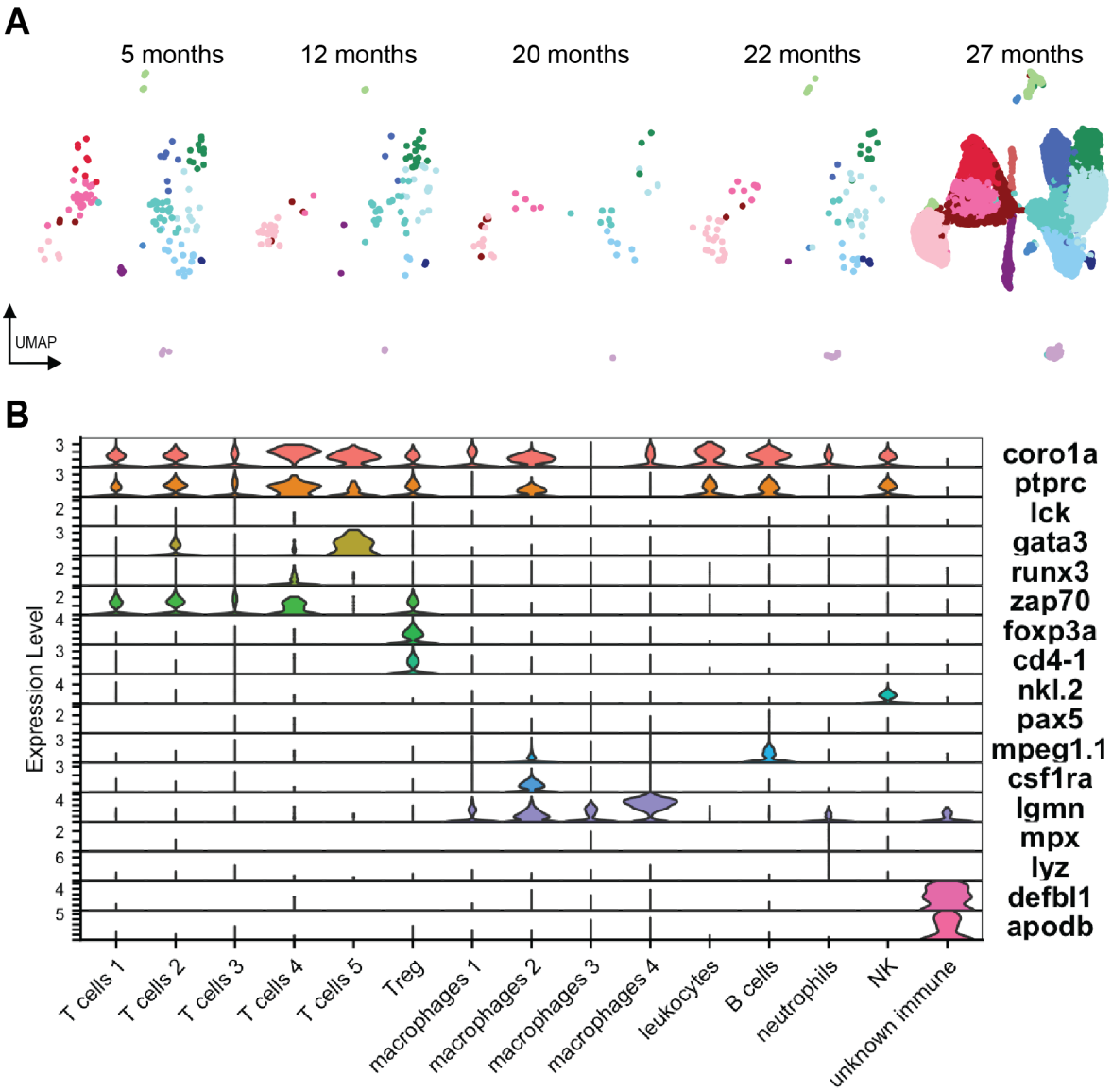

Supplemental Figure 5. Immune atlas.
(A) Immune atlas split by sample age. **(B)** Violin plots show marker genes used to identify each cell type.

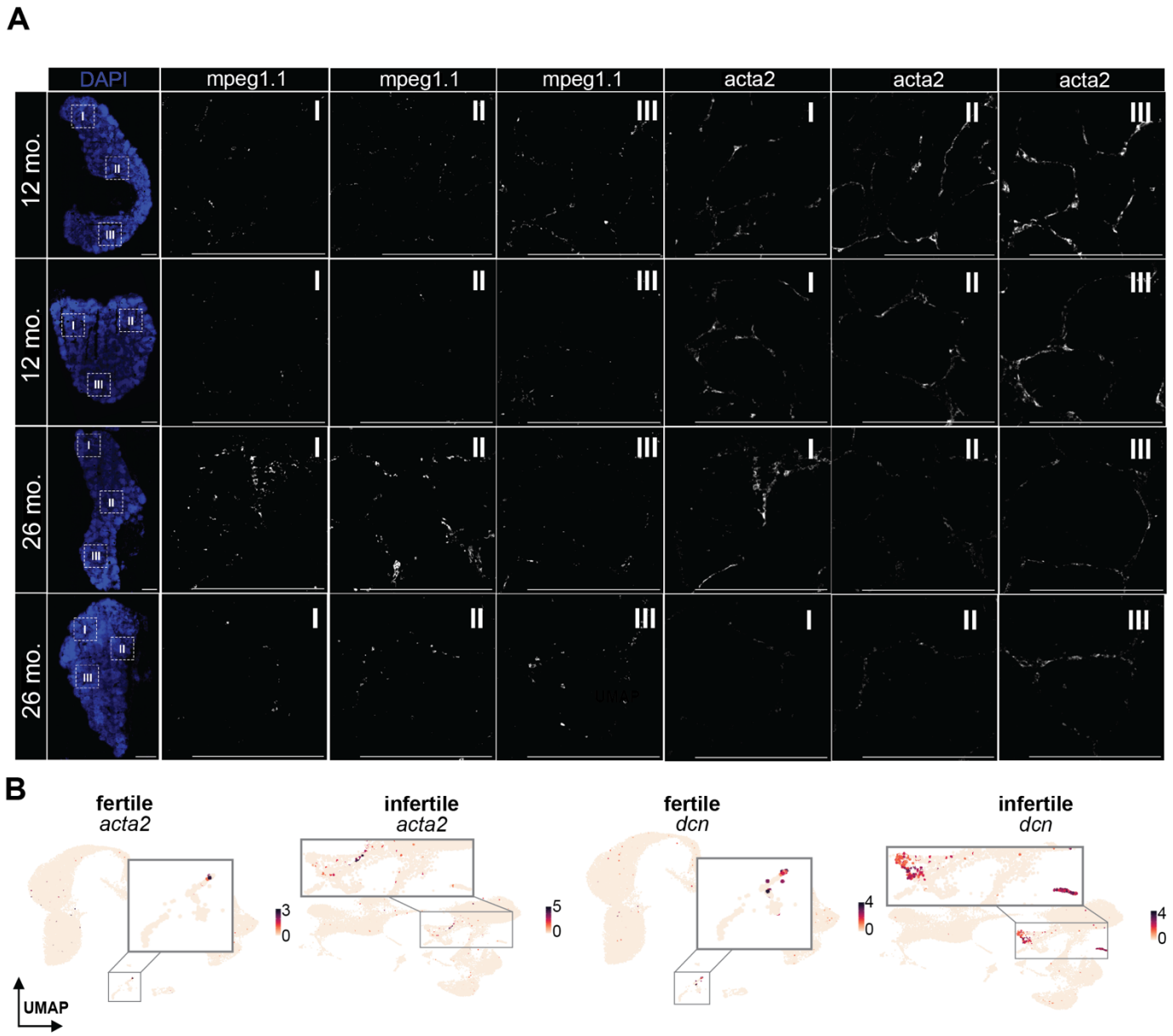

Supplemental Figure 6. RNA in situ hybridization of immune and smooth muscle cells in fertile and infertile testes.

(A) RNAscope of fertile and infertile zebrafish testes. **(B)** Expression of markers *acta2* and *dcn* in fertile and infertile atlases. *Acta2* weakly labels smooth muscle cells. *Dcn*, a marker of stressed vascular endothelial cells and fibroblasts, is expressed more abundantly in infertile testes.

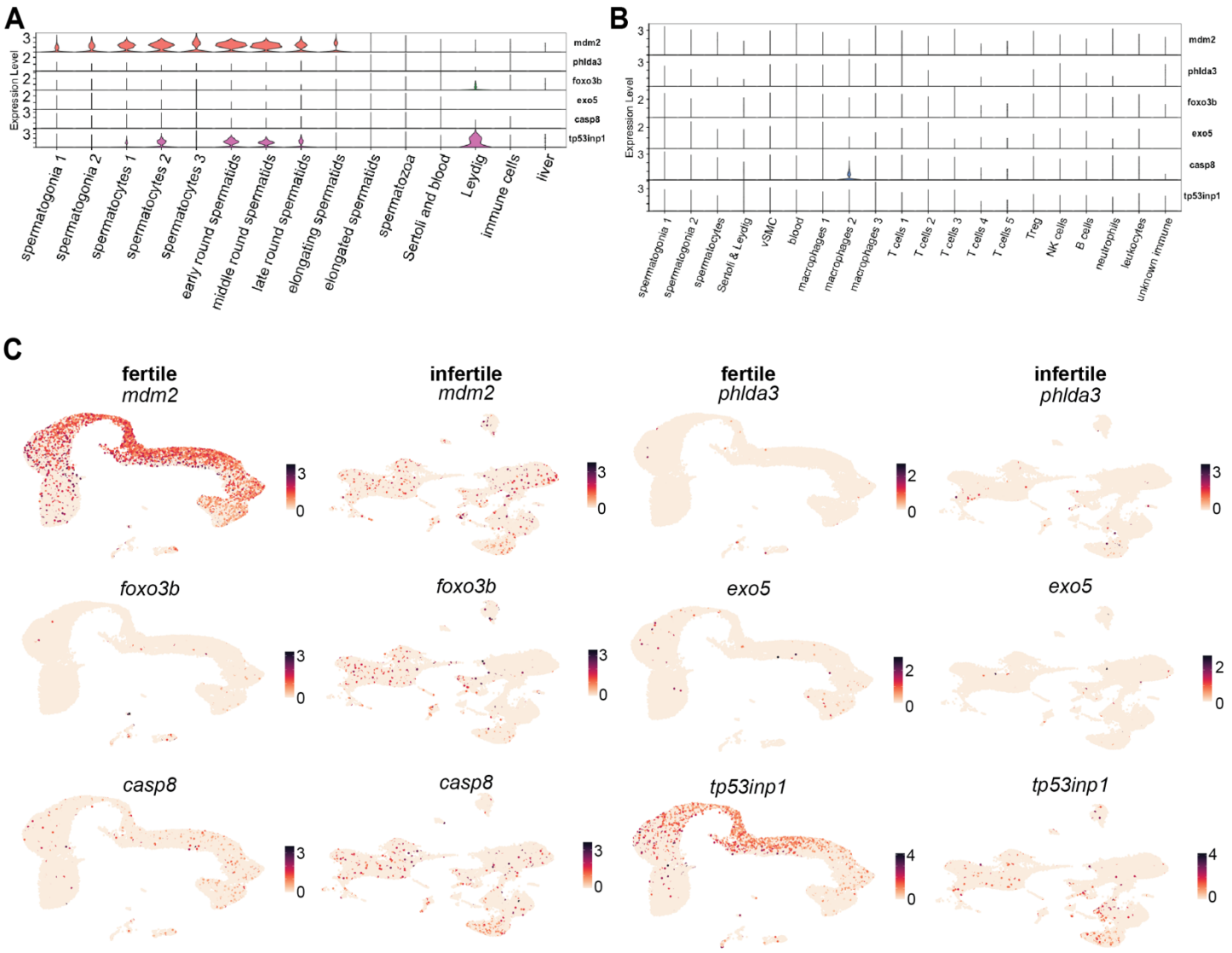

Supplemental Figure 7. Differences in apoptosis between fertile and infertile testes. (A) Violin plots of apoptotic markers in fertile cell types. (B) Violin plots of apoptotic markers in infertile cell types. (C) Expression patterns of apoptotic markers from A and B in both fertile and infertile testes. All markers positively regulate apoptosis except *mdm2* which is an inhibitor.